Dose Optimization and Evaluation of Image Quality in Adult Brain Protocol of Multislice Computed Tomography: A Phantom Study

Thawatchai Prabsattroo *, Kanokpat Wachirasirikul, Prasit Tansangworn, Puengjai Punikhom, Waraporn Sudchai

Posted Date: 7 November 2023

doi: 10.20944/preprints202311.0443.v1

Keywords: dose optimization; iterative reconstruction; image quality; radiation dose

Article

Dose Optimization and Evaluation of Image Quality in Adult Brain Protocol of Multislice Computed Tomography: A Phantom Study

Thawatchai Prabsattroo [1,*], Kanokpat Wachirasirikul [1], Prasit Tansangworn [1], Puengjai Punikhom [1] and Waraporn Sudchai [2]

[1] Department of Radiology, Faculty of Medicine, Khon Kaen University, Thailand; thawatp@kku.ac.th
[2] Nuclear technology service center, Thailand Institute of Nuclear Technology, Thailand
* Correspondence: Thawatchai Prabsattroo; thawatp@kku.ac.th

Abstract: Background: Computed tomography examinations have produced high radiation doses to patients, especially the CT brain. This study aimed to optimize the radiation dose and image quality in adult CT brain protocol. **Materials and Methods:** Images were acquired by Catphan 700 phantom. Radiation doses were recorded as CTDIvol and dose length product (DLP). CT brain protocols were optimized by varying parameters such as kVp, mAs, signal-to-noise ratio (SNR) level, and Clearview iterative reconstruction (IR). Image quality were also evaluataion by The AutoQA Plus software. **Results:** CT Number accuracy and linearity had a robust positive correlation with the linear attenuation coefficient (μ) and showed more inaccurate CT numbers when using 80 kVp. MTF showed a higher value in 100 and 120 kVp protocols, while high contrast spatial resolution showed a higher value in 80 and 100 kVp protocols. Low contrast detectability and CNR tended to increase when using high mAs, SNR and Clearview IR protocol. Noise decreased when using a high radiation dose and a high percentage of Clearview IR. CTDIvol and DLP were increased with increasing kVp, mAs, and SNR levels, while the increasing percentage of Clearview did not affect the radiation dose. **Conclusion:** Optimized protocols, including radiation dose and image quality, should be evaluated to preserve diagnostic capability. The recommended parameter settings include kVp set between 100-120 kVp, mAs ranging from 200-300 mAs, SNR level within the range of 0.7-1.0, and an iterative reconstruction value of 30% Clearview to 60% or higher.

Keywords: dose optimization; iterative reconstruction; image quality; radiation dose

1. Introduction

Computed tomography examinations have produced high radiation doses to patients, especially the CT scan in the brain [1]. Currently, CT machines use various technologies or innovations to reduce the radiation dose to the patients or receive the most negligible radiation dose. In addition, It also tries to use low-radiation protocols and develop algorithms or image processing to improve image quality, resulting in better image quality [2–7]. Usually, CT protocols were established by the Vendor and did not modify or optimize protocols when used for a long time. Image quality and radiation dose were not considered, and realize

In radiation protection principles, optimization is considered an essential process to ensure that patients receive the appropriate amount of radiation for the examination and that image quality is sufficient for diagnosis [8–11]. Computed tomography (CT) is a diagnostic imaging modality that uses high radiation doses to create images and may expose the patient to radiation risk [12,13]. CT scans of the head expose sensitive organs, especially the lens of the eyes, which can be damaged and cause cataracts if the radiation dose exceeds a certain level [13–17].

According to a report by the United States and Canada, CT scan machines have been widely used in many countries and contribute radiation dose to patients approximately 24.2% of all doses received in daily life [1,18]. Many parameters affect radiation to the patient, such as kVp, mA, mAs,

 doi:10.20944/preprints202311.0443.v1

pitch, scan range, slice thickness, and reconstruction algorithm. Acquisition parameters also affect image quality and performance of images for diagnosis [15,19–22].

Objective and subjective evaluation methods could analyze image quality in CT images [23–26]. In the objective evaluation method, images are evaluated and quantitatively using the QA CT phantom or CT image of the patient. The subjective evaluation method evaluated the image quality by radiologists or experts and scored the image quality. The typical quantitative parameters are used to evaluate the image quality, including CT number accuracy and linearity, high-contrast spatial resolution, modulation transfer function (MTF), low-contrast detectability and contrast-to-noise ratio (CNR), image noise, uniformity and mean CT number [27,28].

Optimization protocol should balance radiation and image quality because acquisition parameter changes could affect image quality. Therefore, the objectives of this study were to optimize the CT brain protocols by varying kVp, mAs, SNR, and Clearview iterative reconstruction (IR) algorithm and evaluate image quality by the qualitative method using Catphan700 phantom to obtain the image. Image quality evaluation used AutoQA Plus software and showed as CT number accuracy and linearity, high-contrast spatial resolution, modulation transfer function (MTF), low-contrast detectability and contrast-to-noise ratio (CNR), image noise, uniformity and mean CT number.

2. Materials and Methods

This study used a Catphan700 phantom to acquire images and CT scanner was Neusoft in a model of NeuViz 128 (Neusoft Medical Systems, Shenyang, China) with 128 slices. The optimized protocols were adjusted by varying kVp, mAs, SNR, and Clearview iterative reconstruction. After finishing the scanning, a radiation dose of CT was recorded as CTDIvol and DLP.

2.1. Image acquisition protocols

The scan parameters were presented in Table 1. All CT scanners were performed with the same scan parameters, and all data acquisitions were performed 3 consecutive times.

Table 1. Data acquisition protocols used for dose optimization in default clinical brain protocols of Neusoft NeuViz 128 CT scanner.

Parameters	Default (Optimized protocol)
kVp	120 (80, 100, 140)
mAs	300 (100, 200, 400)
Rotation time	1.0 s
Pitch	0.5
Slice thickness	5 mm
SNR Level	1.0 (0.3, 0.7, 1.3, 1.7)
FOV	250 mm
Kernel	F20
IR	50% (20%, 30%, 40%, 60%) Clearview
Matrix	512*512

2.2. Data acquisition and image quality evaluation

The Catphan 700 phantom was used to acquire the image by scanning according to three clinical routine scans for the brain, chest, and whole abdomen with three different CT scanners from various manufacturers. The AutoQA Plus software (QA Benchmark, LLC), was used to analyze image quality.

2.3. Catphan 700 phantom

A Catphan 700 phantom (The Phantom Laboratory Incorporated, Salem, NY, USA) was used to evaluate all image quality [29,30]. The phantom has a cylindrical shape and contains 6 modules including CTP682; geometry sensitometry and point source module, CTP714; 30-line pair high-

 doi:10.20944/preprints202311.0443.v1

resolution module, CTP515; subslice and supra-slice low contrast, CTP721; wave insert, CTP723; bead blocks, and CTP712; uniformity section. CT scanners of the Catphan phantom were obtained by Neusoft NeuViz 128 (Neusoft Medical Systems, Shenyang, China) [31]. Quality control (QC) testing was performed annually for all CT scanners and the CT number was also calibrated.

2.4. CT number accuracy and linearity

The module CTP682 containing different sensitometry targets was used to perform CT number accuracy and linearity [32–34]. This module has sensitometry targets made from Teflon®, Bone 50%, Delrin®, Bone 20%, acrylic, Polystyrene and low-density polyethylene (LDPE), polymethylpentene (PMP), Lung foam #7112, and air including a water container. In the circular region of interest (ROI), approximately 80% of each target size was selected and the measured mean CT number was recorded for each target. The mean CT number of each target was compared to the range of actual CT numbers from the specifications of phantom. The linearity was also tested using Pearson's correlation coefficient (r) between the measured CT number and each target's linear attenuation coefficients (μ). CT numbers accuracy should not exceed the tolerance limit from the recommendation range of Catphan 700 phantom.

2.5. The high-contrast spatial resolution and modulation transfer function (MTF)

High-contrast spatial resolution is the ability of a system to distinguish high-contrast objects from neighboring objects [35]. Two broad methods exist to analyze high-contrast spatial resolution by calculating the modulation transfer function (MTF) and objective analysis or resolution bar pattern assessment [35–37]. The spatial resolution is measured by calculating a small wire's point spread function (PSF) with 0.05 mm tungsten (module CTP682). PSF generates line spread functions (LSF) in both vertical and horizontal directions. The MTF was calculated by taking the Fourier transform and showed in the value line pair/cm at 50%, 10%, and 2% of the MTF. The CTP714 High-resolution module with 1-30 line pair per cm gauges was used to evaluate high resolution. The tolerance levels of spatial resolution in the CT brain should exceed 5 lp/cm [34]. The expected values of MTF at 50%,10%, and 2% exceeded 3, 5, and 7 cycles/cm, respectively [29,38,39].

2.6. Low-contrast detectability and contrast-to-noise ratio (CNR)

Low contrast resolution refers to the ability of a system to distinguish between low-contrast structures and their background [6,32,40,41]. Module CTP515 was used to determine CNR which contains low contrast supra slice targets with diameters of 15, 9, 8, 7, 6, 5, 4, 3, and 2 mm, and contrast levels of 0.3%, 0.5%, and 1.0%. CNR measured the difference between target signals and background signals. Low contrast detectability was also calculated and shown as the theoretical Contrast-Detail curve. The curve showed the minimum contrast level at the given diameter that should be visible. CNR performance should meet the standards at 1 for adult head protocol [32].

2.7. Image noise, uniformity and mean CT number

The CTP71 was used for the measurement of uniformity and image noise[29,32,34,42]. Image uniformity was measured by using the difference value of the maximum HU of the center and the 4 peripheral ROI at 3, 6, 9, and 12 O'clock locations. The noise level was defined as SD and measured at the center with a diameter of ROI 40% of the phantom. The mean CT number represents the center ROI mean for a phantom's 10% ROI size. The difference between the mean CT value of each peripheral ROI and the center ROI should not exceed 5 HU and the noise level should not exceed 5 [32]. The mean CT number should not exceed 12±10 HU.

2.8. Radiation dose

The CTDIvol and Dose length product (DLP) were used as dose indices for CT and collected from dose report. The DLP is calculated by multiplying the CTDIvol by the scan length [21,43].

 doi:10.20944/preprints202311.0443.v1

2.9. Statistical analysis

Quantitative data from image quality evaluation and radiation dose were expressed as mean. CT number linearity was tested by using Pearson's correlation. CT accuracy was compared with the tolerance values of recommendation. The parameters for the evaluation of image quality were analyzed by AutoQA Plus software and compared with the default protocol or the reference and tolerance values of the American College of Radiology (ACR) or the International Electrotechnical Commission (IEC). Radiation doses (CTDIvol, DLP) were compared with the default protocol and the percentage difference from the default protocol was also calculated.

3. Results

3.1. CT Number accuracy

Table 2 found that the correlation coefficient was between 0.998165 and 0.999701. It indicates that CT numbers and linear attenuation coefficients have a very high positive relationship. For default clinical brain protocol at 120 kVp, 300 mAs, SNR 1.0, and 50% Clearview IR algorithm showed that CT numbers did not pass the evaluation criteria for Teflon and Delrin. When the kVp was changed to 80 kVp, Acrylic, Bone 50%, LDPE, Bone 20%, Polystyrene, and PMP did not pass the criteria, while Teflon and Delrin did not pass the criteria at 100 kVp. At 140 kVp, Bone 20%, and Delrin did not pass the criteria. When the mAs were changed to 100, 200, and 400 mAs, with SNR levels of 0.3, 0.7, 1.3, and 1.7, and 20%, 30%, 40%, and 60% Clearview IR, Teflon and Delrin did not pass the criteria.

Table 2. CT number accuracy in each optimized protocol and material and correlation coefficient (r) showed the relationship between CT Number and attenuation coefficient.

Materials	80 kVp 300 mAs	100 kVp 300 mAs	120 kVp 300 mAs (Default)	140 kVp 300 mAs	120 kVp 100 mAs	120 kVp 200 mAs	120 kVp 400 mAs	
Air	-973.8	-971.9	-967.8	-968	-968	-968	-969.1	
Lung	-806.5	-805.1	-798.5	-800.3	-798.4	-800	-800	
PMP	-211.2	-190.8	-177.1	-171.1	-176.5	-176.6	-176.5	
LDPE	-123.9	-103.7	-90	-82.1	-89.1	-88.8	-89	
Polystyrene	-67.5	-46.9	-33.6	-27.7	-34.7	-33.3	-33.8	
Water	-0.9	1.3	2.8	0.7	3.5	3.5	3.3	
Acrylic	98.5	112.6	122.6	127.1	123.5	124.6	123.3	
Bone20	302	168.5	186.9	223.6	186.2	187.1	187.5	
Delrin	330.4	244.7	301.1	360.9	300.3	301.3	301.1	
Bone50	908.3	643.1	629.9	636	628.2	631	629	
Teflon	969	813.5	882	931.1	882.4	882.1	883.1	
r	0.998165	0.998533	0.999676	0.999695	0.999676	0.999655	0.999668	
Materials	**SNR 0.3**	**SNR 0.7**	**SNR 1.3**	**SNR 1.7**	**20% Clearview**	**30% Clearview**	**40% Clearview**	**60% Clearview**
Air	-969.6	-968.6	-966.7	-967.6	-969.9	-969.6	-970.2	-965.3
Lung	-800.5	-799.4	-798.3	-797.8	-800.7	-799.7	-801.5	-797.8
PMP	-177.5	-176.9	-177.4	-176.5	-176.6	-176.9	-177.5	-175.9
LDPE	-90.8	-89.3	-88.8	-89.2	-89.3	-89.9	-89.7	-89.6
Polystyrene	-35.5	-34.7	-33.9	-34.3	-34.6	-34.5	-35	-33.6
Water	2.2	2.5	1.8	2.6	2.7	3.7	1.4	3.2
Acrylic	122.6	124.1	123.3	123.8	123.6	123.2	123	123.3
Bone20	188.8	186.4	187.7	188.3	188.8	189.1	187.8	184
Delrin	300.4	299.8	300.1	300	299.3	300.7	299.7	300.8
Bone50	628.6	629.3	628.1	629.1	628.6	628.8	628.4	628.3

Preprints (www.preprints.org) | NOT PEER-REVIEWED | Posted: 7 November 2023 doi:10.20944/preprints202311.0443.v1

Teflon	881.6	881.7	879.7	880.4	882.4	881.1	879.9	882.7
r	0.999656	0.999657	0.999653	0.999647	0.999636	0.999646	0.999636	0.999701

3.2. Modulation transfer function: MTF

All optimized protocols demonstrated that the MTF passed the evaluation criteria for all percentages of MTF at 50%, 10%, and 2%, with tolerance levels of 3, 5, and 7 cycles/cm, respectively (Table 3). MTF by varying kVp revealed that protocols at 100 and 120 kVp had MTF that was 50%, 10%, and 2% higher than protocols at 80 and 140 kVp. When the mAs were optimized to 100, 200, 300, and 400 mAs, it was found that the MTF values at 50%, 10%, and 2% showed a higher MTF when the mAs were increased. When the SNR levels were varied to 0.3, 0.7, 1.0, 1.3, and 1.7, it was found that the MTF value increased as the SNR level increased. Finally, the IR at 20%, 30%, 40%, 50%, and 60% Clearview was discovered that the MTF value showed a similar value of MTF at 30%, 40%, 50%, and 60% Clearview, while 20% MTF showed the worst MTF.

Table 3. MTF at 50 %, 10%, and 2% of optimized protocols.

MTF (%)	**80 kVp 300 mAs**	**100 kVp 300 mAs**	**120 kVp 300 mAs (Default)**	**140 kVp 300 mAs**	**120 kVp 100 mAs**	**120 kVp 200 mAs**	**120 kVp 400 mAs**	
50	3.74	4.37	4.18	3.86	4.03	4.28	4.5	
10	6.85	7.07	7.1	6.69	6.97	6.97	6.97	
2	8.33	8.34	8.82	8.41	8.09	8.09	8.31	
MTF (%)	**SNR 0.3**	**SNR 0.7**	**SNR 1.3**	**SNR 1.7**	**20% Clearview**	**30% Clearview**	**40% Clearview**	**60% Clearview**
50	4.41	4.41	4.41	4.41	3.95	4.12	4.12	4.29
10	6.87	6.93	6.94	7.02	6.83	6.95	7.12	7.12
2	8.45	8.5	8.52	8.62	8.54	8.55	8.59	8.59

3.3. High Contrast spatial resolution

Figure 1 showed that the 80 kVp and 100 kVp protocols had higher high-contrast spatial resolution than the 120 kVp and 140 kVp protocols. The mAs, SNR, and percent Clearview IR algorithm did not affect the high-contrast spatial resolution.

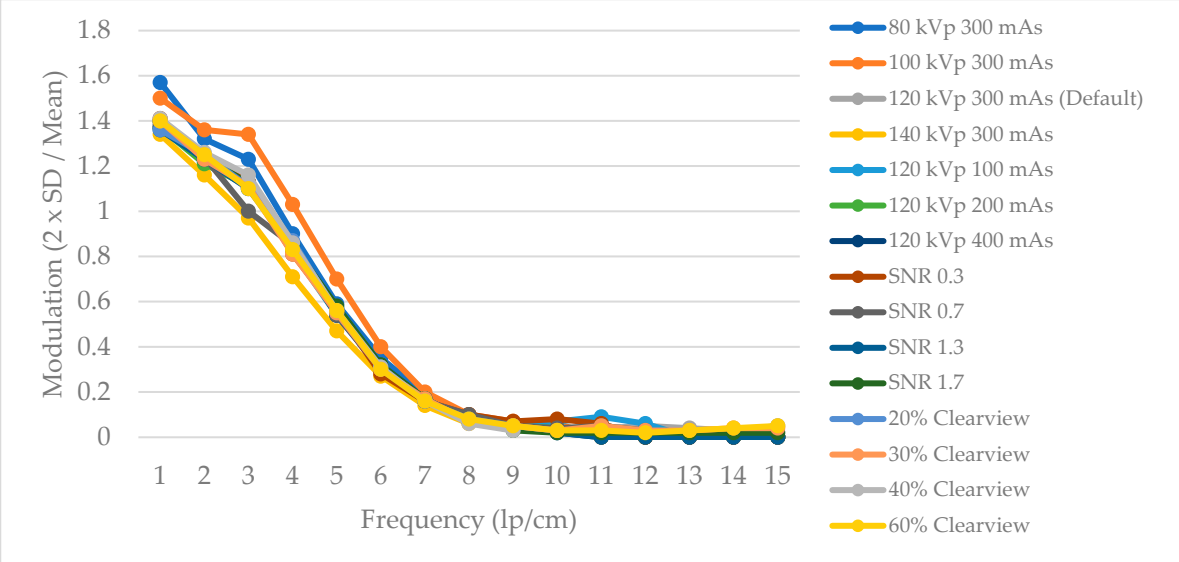

Figure 1. High-contrast spatial resolution of optimized protocols.

Preprints (www.preprints.org) | NOT PEER-REVIEWED | Posted: 7 November 2023 doi:10.20944/preprints202311.0443.v1

3.4. Low contrast detectability

Figure 2 showed low contrast detectability in C-D model. It was found that increasing kVp, mAs, SNR, and % Clearview IR exhibited the improvement of low contrast detectability in the low contrast object and small diameter of the object. In contrast, decreasing kVp, mAs, SNR, and % Clearview IR showed a decrease in low contrast detectability.

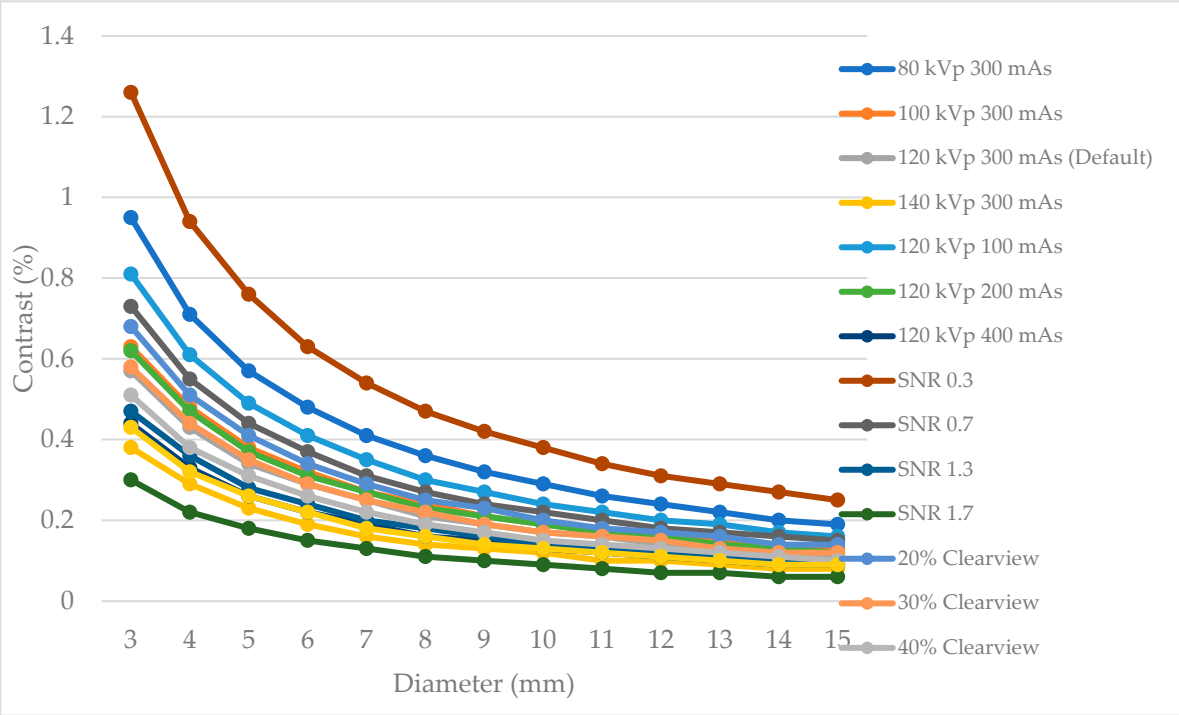

Figure 2. Low contrast detectability of optimized protocols.

3.5. Contrast to noise ratio: CNR

Figures 3–5 showed CNR at percent contrast objects at 1%, 0.5%, and 0.3 % with various object diameters. It was found that increasing radiation dose by increasing kVp, mAs, and SNR showed higher CNR, especially protocols of SNR 1.7 and SNR 1.3. Increasing % Clearview IR also showed a higher CNR. In contrast, decreasing radiation via decreased kVp, mAs, and SNR showed a decrease in low contrast detectability. The higher % Clearview IR showed an improvement in CNR.

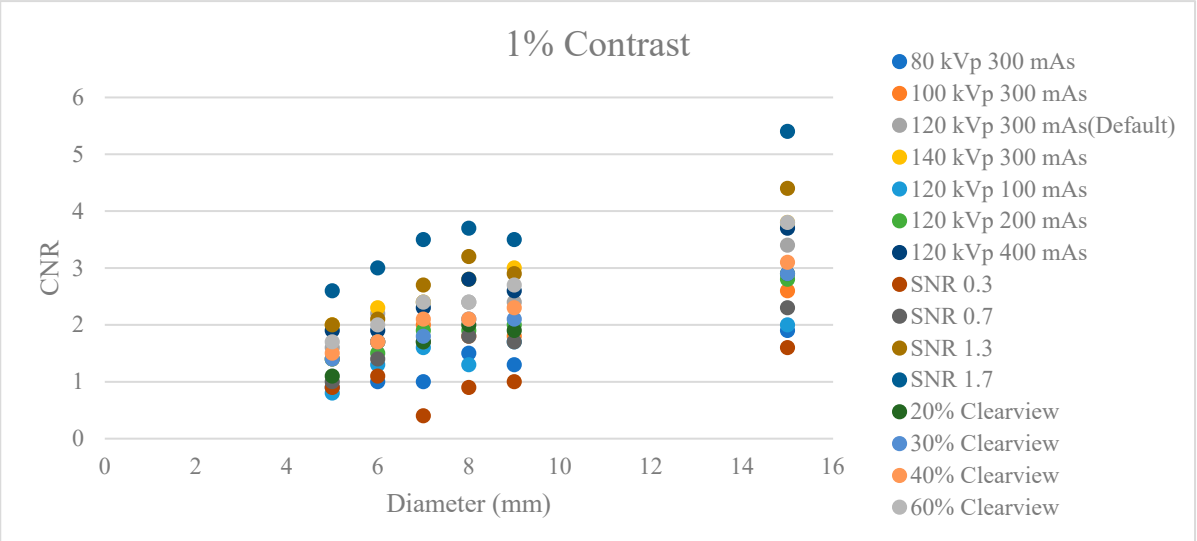

Preprints (www.preprints.org) | NOT PEER-REVIEWED | Posted: 7 November 2023 doi:10.20944/preprints202311.0443.v1

Figure 3. Contrast to noise ratio at 1% Contrast with various diameters of optimized protocols.

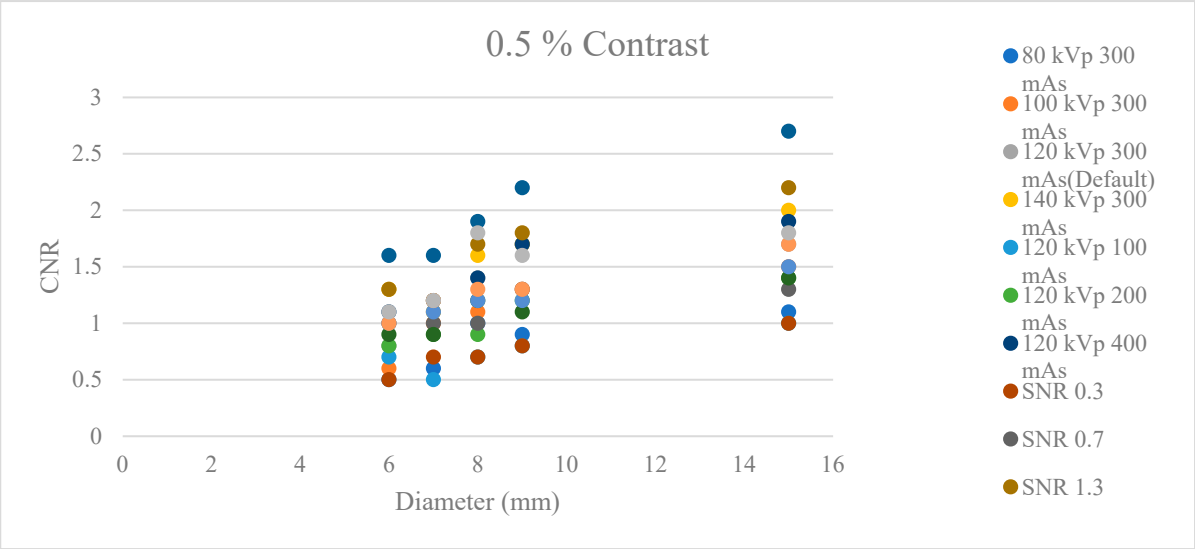

Figure 4. Contrast to noise ratio at 0.5 % Contrast with various diameters of optimized protocols.

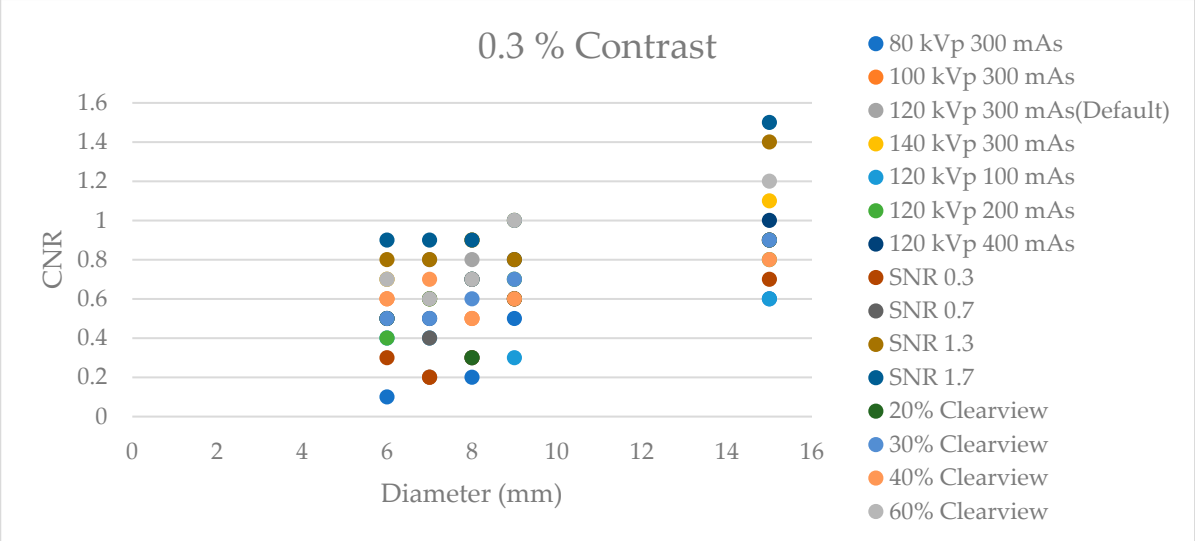

Figure 5. Contrast to noise ratio at 0.3 % Contrast with various diameters of optimized protocols.

3.6. Image Noise, Uniformity, and mean CT number

Figure 6 showed noise levels from various optimized protocols. Noise levels were found to be acceptable within a tolerance of 5 HU for protocols of 120 kVp, 140 kVp, 200 mAs, 400 mAs, SNR 0.7, SNR 1.3, SNR 1.7, and all percent Clearview IR algorithm. Figure 7 showed that all protocols failed to meet the acceptable range of 4 HU. Figure 8 demonstrated that the mean CT number of all protocols was within the acceptable range of 12±10 HU except for protocol 80 kVp, which had a low mean CT number.

Preprints (www.preprints.org) | NOT PEER-REVIEWED | Posted: 7 November 2023 doi:10.20944/preprints202311.0443.v1

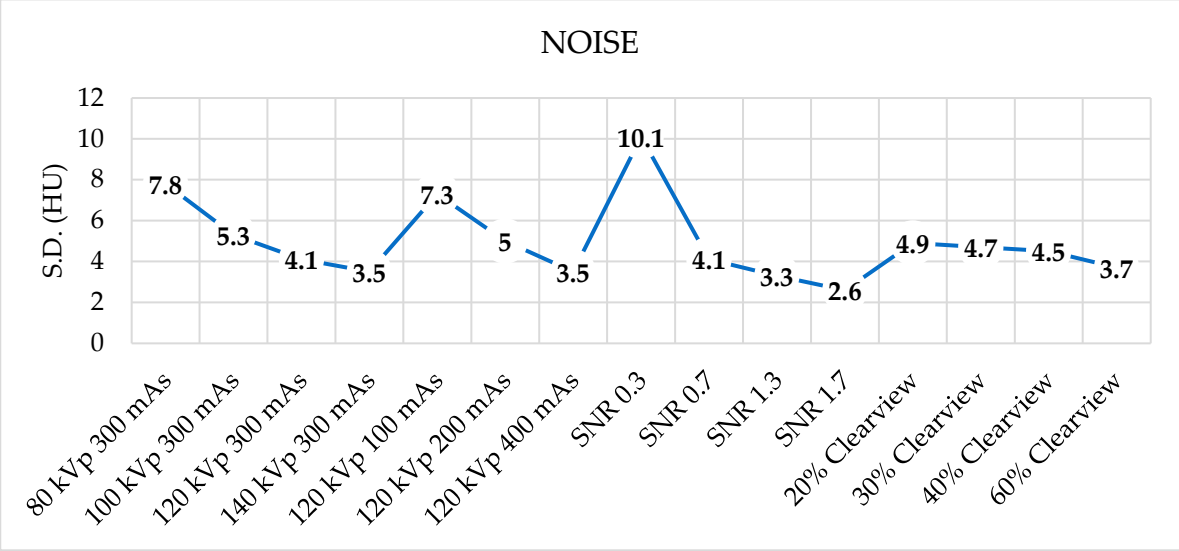

Figure 6. Noise level of optimized protocols.

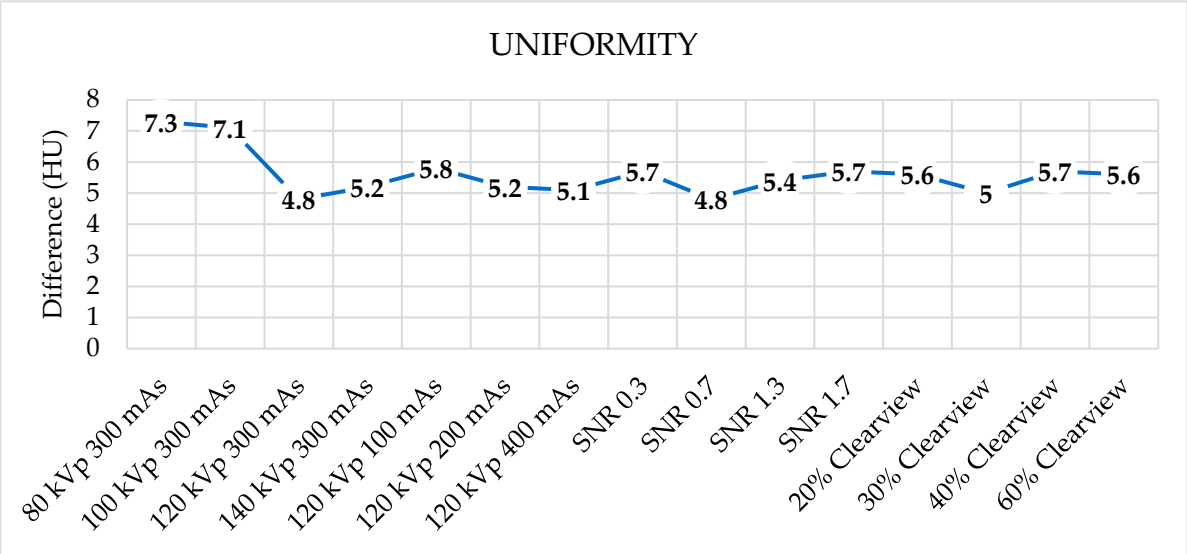

Figure 7. Uniformity of optimized protocols.

Preprints (www.preprints.org) | NOT PEER-REVIEWED | Posted: 7 November 2023 doi:10.20944/preprints202311.0443.v1

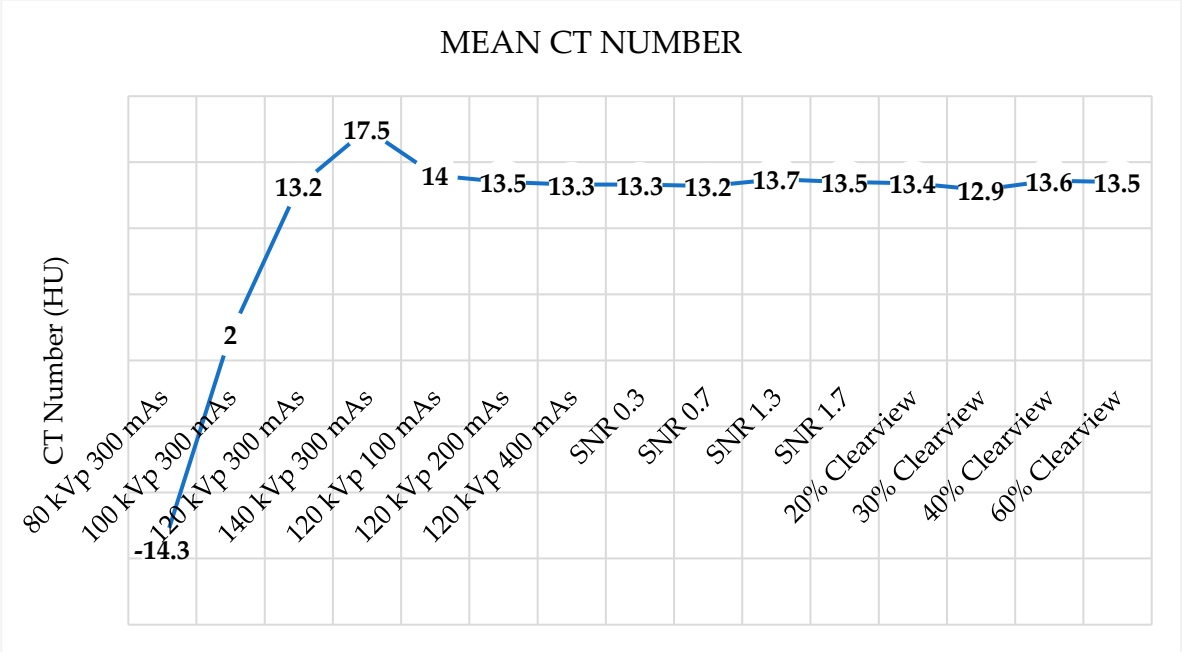

Figure 8. Mean CT Number of optimized protocols.

3.7. Radiation Dose

Figures 8 and 9 showed CTDIvol and DLP of optimized protocols. The default clinical protocol of CT brain exhibited CTDIvol and DPL at 37.2 mGy and 827.4 mGy*cm, respectively. It was found that protocols of 80 kVp, 100 kVp, 100 mAs, 200 mAs, SNR 0.3, and SNR 0.7 were lower CTDIvol and DPL than the default clinical protocol. While 140 kVp, 400 mAs, SNR 1.3, and SNR 1.7 showed higher CTDIvol and DLP than the default clinical protocol. CTDIvol and DLP did not affect when the levels of the Clearview IR algorithm changed. Table 4 showed the percentage difference of CTDIvol and DLP compared to the default clinical protocol. The lower CTDIvol and DPL protocol could decrease CTDIvol to 33.3% - 80.1% mGy and DLP to 33.4% - 80.4% mGy*cm. A higher dose protocol could increase CTDIvol to 33.6% - 147.6% mGy and DLP to 30.3% - 141.8% mGy*cm.

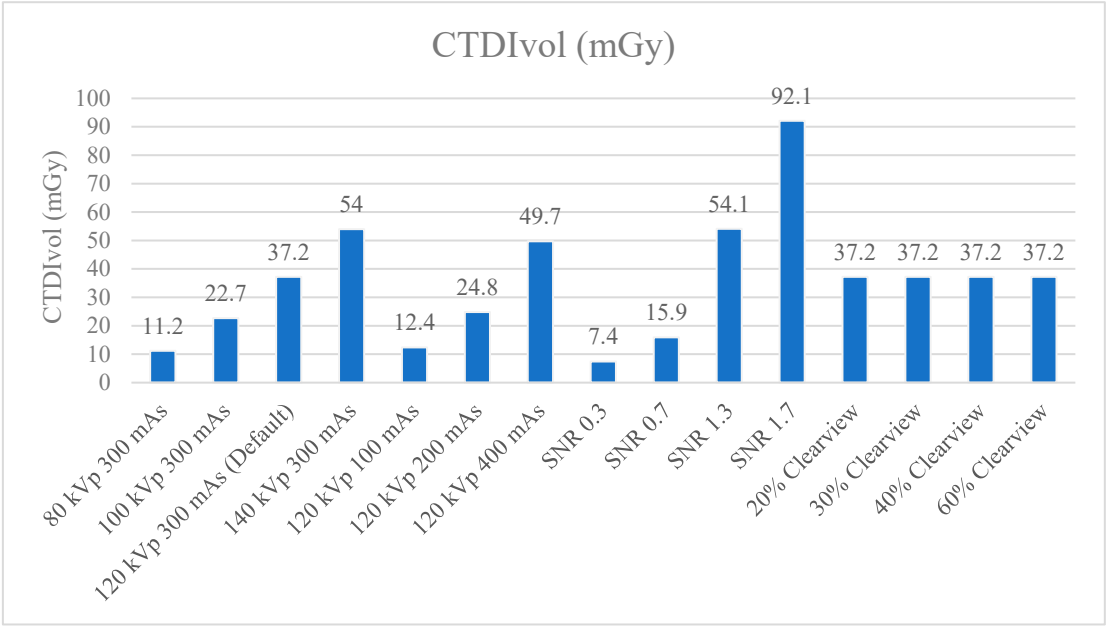

Figure 8. CTDI$_{vol}$ (mGy) of optimized protocols.

Preprints (www.preprints.org) | NOT PEER-REVIEWED | Posted: 7 November 2023 doi:10.20944/preprints202311.0443.v1

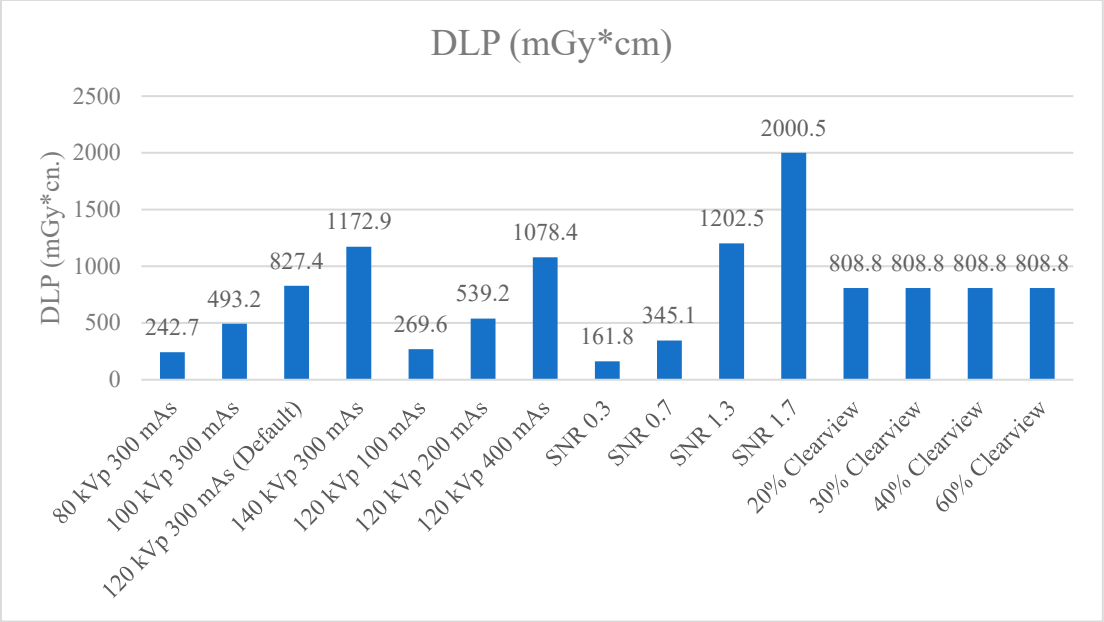

Figure 10. DLP (mGy*cm) of optimized protocols.

Table 4. Percentage difference of CTDIvol and DLP compared to default clinical protocol.

	80 kVp 300 mAs	100 kVp 300 mAs	120 kVp 300 mAs (Default)	140 kVp 300 mAs	120 kVp 100 mAs	120 kVp 200 mAs	120 kVp 400 mAs	
% Diff of CTDIvol	-69.9	-39.0	0.0	45.2	-66.7	-33.3	33.6	
% Diff of DLP	-70.7	-40.4	0.0	41.8	-67.4	-34.8	30.3	
	SNR 0.3	SNR 0.7	SNR 1.3	SNR 1.7	20% Clearview	30% Clearview	40% Clearview	60% Clearview
% Diff of CTDIvol	-80.1	-57.3	45.4	147.6	0.0	0.0	0.0	0.0
% Diff of DLP	-80.4	-58.3	45.3	141.8	0.0	0.0	0.0	0.0

4. Discussion

Optimization is considered an essential process in the principles of radiation protection to ensure that patients receive the appropriate amount of radiation for the examination and that image quality is sufficient for diagnosis. Computed tomography (CT) is one of the diagnostic imaging modalities that uses high radiation doses to form images and may contribute to radiation risk to the patient. CT scans of the head expose sensitive organs, particularly the lens of the eyes, which may be damaged and cause cataracts if the radiation dose exceeds a certain threshold. This study aimed to optimize the protocol for CT brain scans, a routine protocol used in clinical practice. The protocol was adjusted with the following scanning parameters: kVp (80, 100, 120, 140), mAs (100, 200, 300, 400), SNR (0.3, 0.7, 1, 1.3, 1.7), and Iterative Reconstruction algorithm (20%, 30%, 40%, 50%, 60% Clearview). Moreover, quantitative image quality was also evaluated using the Catphan700 phantom to acquire images and evaluated the CT number accuracy and linearity, MTF, high contrast spatial resolution, low contrast detectability, CNR, image noise and uniformity, and mean CT number. CTDIvol and DLP values were also recorded and evaluated in various adjusted brain protocols.

The results demonstrated that CT Number accuracy was within the specified range for most materials and showed a linear relationship between each material's linear absorption coefficient (μ) and CT number. The correlation coefficient (*r*) was within the range of 0.998165 to 0.999701, showing a strong positive relationship. For the 80 kVp protocol adjustment, it was found that the CT Number

 doi:10.20944/preprints202311.0443.v1

accuracy showed out-of-range CT numbers in many materials because the average energy was decreasing, affecting the absorption coefficient (μ), resulting in the CT number increasing[33]. Usually, 120 kVp is regularly used for CT scans, and this machine has an effective energy of approximately 60 keV. Reducing the energy to 80 kVp will affect average energy and CT number accuracy. Besides, the factors affecting the CT number accuracy depend on the filter and patient thickness[44,45]. Therefore, CT number measurement for diagnosis should be considered carefully because of the high error of CT number 6. Some materials in another protocol also showed an error of CT number accuracy. It has been recommended that water calibration should be performed regularly to help maintain the accuracy of CT numbers, especially the CT number accuracy of water material [46].

High-contrast spatial resolution is used to distinguish small objects with high contrast. It can be measured in two ways by MTF and high-resolution bar patterns. MTF values of 50%, 10% and 2% of all protocols were found to have passed the 3 lp/cm, 5 lp/cm, and 7 lp/cm benchmark, respectively. The results demonstrated MTF of the 80 and 140 kVp protocol showed lower MTF than 100 and 120 kVp because of increasing noise at 80 kVp and the scatter radiation at 140 kVp [47]. Increasing mAS and SNR could increase radiation, resulting in low noise levels. 20 % Clearview IR showed the worst MTF because the power of IR at 20 % was not good enough to improve image quality. High-resolution assessments using bar patterns at 80 and 100 kVp protocols showed higher high-contrast spatial resolution because lower kVp could increase the high-contrast resolution of images. According to the previous study, the factors affecting MTF and spatial resolution were not only reconstruction algorithms but also detector width, effective slice thickness, object-to-detector distance, X-ray tube focal spot size, and matrix size. These factors also affect MTF and spatial resolution [48,49]. The Research of Yali Li et al. found that 10% of MTF was 6.98±0.40 lp/cm, correlating with subjective assessment showing 7 lp/cm. Moreover, Clearview is suitable for low-dose protocols because it reduces noise and artifacts [40]

Low contrast detectability is the ability to separate low-contrast objects from the background. It was found that protocols that use low radiation doses tend to have decreased low-contrast resolution such as SNR 0.3 protocol, 80 kVp protocol, and 100 kVp protocol. The protocols with improved low-contrast resolution were SNR 1.7 protocol, 140 kVp protocol, and 60% Clearview protocol. In addition, it was found that the CNR value decreased with the percentage contrast of the object decrease and the small diameter of the object. A study by Manson EN et al. and Gulliksrud K et al. showed that noise was an essential factor that reduced low-contrast resolution and CNR [50,51]. Moreover, higher radiation dose protocols and a higher percentage of reconstruction algorithms could improve low-contrast resolution and CNR [50].

The evaluation of image uniformity was to measure the stability of the CT number by comparing the CT number values in the center of the phantom with the peripheral edges of the phantom. It was found that the uniformity of the images was not within the criteria specified in every protocol, with values exceeding ±4 HU. Noise is the average of the standard deviation (SD) measured at the center of the phantom. Protocols that use high radiation doses such as high mAs, high kVp and high IR % Clearview tend to decrease noise. Research Yali Li et al found that the protocol that increased radiation dose and iterative reconstruction algorithm reduced noise and improved image quality[40].

CTDIvol and DLP were used to evaluate radiation dose and be a dose index in the CT. CT has been conducting quality control annually to measure CTDIvol and the value shown in the CT display was not different from the acceptable threshold of ±20%. The DLP value obtained from CTDIvol multiplied by scan length according to the clinical default protocol of CT brain shows 37.2 mGy of CTDIvol. Increasing mAs, kVp, and SNR showed a higher CTDIvol while increasing the percentage of the Clearview IR algorithm did not affect CTDIvol, but it affected image quality [41,52]. The research of Ozdil Baskan et al. [2] demonstrated that many parameters approached to reduce the radiation dose, such as kVp, mAs, automated tube current modulation, adaptive dose collimation, and appropriate noise-reduction reconstruction algorithms. Adjusting such parameters will affect the image quality; therefore, adjusting the parameters should be considered.

 doi:10.20944/preprints202311.0443.v1

Because this study was carried out on a Catphan phantom, CT images of patients should also be analyzed. Furthermore, optimization was performed in one CT machine from a specific manufacturer; the optimization parameter, algorithm, and image quality result could differ if another manufacturer were used. We proposed that this research be conducted in the CT brain's low-dose protocol to evaluate the performance of the Clearview IR algorithm for noise reduction. Other parameters that affect radiation dose and image quality could be investigated, and radiologists' subjective evaluations should be included for the overall image quality evaluation.

5. Conclusions

The default clinical brain protocol should be optimized for image quality and radiation dose balance. kVp should be set between 100 and 120 kVp because adjusting the kVp below 100 kVp results in a large discrepancy in the CT Number. The mAs should be in the range of 200 - 300 mAs, whereby adjusting the mAs value to 200 mAs will reduce the radiation dose, but the image quality in CNR and low contrast detectability will be similar to the default brain protocol. SNR level should be in the range of 0.7-1.0, whereby adjusting the SNR level to 0.7 will reduce the radiation dose but result in the CNR, Low contrast detectability, and noise within an acceptable range. However, the value of uniformity increases. Iterative reconstruction should be adjusted to a value between 30% Clearview - 60% Clearview or more. Adjusting Clearview to 30% or more will result in CNR, low contrast detectability, and noise reduction without affecting radiation dose. However, noise and non-uniformity of CT images increased when using low-dose protocols.

Author Contributions: Conceptualization, Prabsattroo T.; methodology, Prabsattroo T., Wachirasirikul K. and Tansangworn P.; software, Prabsattroo T., Sudchai W; validation, Prabsattroo T.; formal analysis, Prabsattroo T., Wachirasirikul K. and Tansangworn P.; investigation, Prabsattroo T., Wachirasirikul K. and Tansangworn P.; resources, Punikhom P.; data curation, Prabsattroo T. , Sudchai W.; writing—original draft preparation, Prabsattroo T., Wachirasirikul K. and Tansangworn P.; writing—review and editing, Prabsattroo T.; visualization, Prabsattroo T., Wachirasirikul K. and Tansangworn P; supervision, Prabsattroo T.; project administration, Prabsattroo T. All authors have read and agreed to the published version of the manuscript.

Funding: This research received no external funding.

Institutional Review Board Statement: Not applicable.

Informed Consent Statement: Not applicable.

Data Availability Statement: Not applicable.

Conflicts of Interest: The authors declare no conflict of interest.

Abbreviations

CNR, contrast-to-noise ratio; CT, computed tomography; HU, Hounsflied units; keV, kiloelectronvolt; kVp,kilovolt peak; DLP,dose length product; SNR, signal-to-noise ratio; IR, iterative reconstruction;MTF, modulation transfer function.

References

1. Baselet B, Rombouts C, Benotmane AM, Baatout S, Aerts A. Cardiovascular diseases related to ionizing radiation: The risk of low-dose exposure. International Journal of Molecular Medicine. 2016;38(6):1623–41.
2. Baskan O, Erol C, Ozbek H, Paksoy Y. Effect of radiation dose reduction on image quality in adult head CT with noise-suppressing reconstruction system with a 256 slice MDCT. Journal of applied clinical medical physics. 2015;16(3):285–96.
3. Wang R, Schoepf UJ, Wu R, Reddy RP, Zhang C, Yu W, et al. Image quality and radiation dose of low dose coronary CT angiography in obese patients: sinogram affirmed iterative reconstruction versus filtered back projection. European journal of radiology. 2012;81(11):3141–5.
4. Wichmann JL, Hardie AD, Schoepf UJ, Felmly LM, Perry JD, Varga-Szemes A, et al. Single-and dual-energy CT of the abdomen: comparison of radiation dose and image quality of 2nd and 3rd generation dual-source CT. European radiology. 2017;27(2):642–50.

5. Schuhbaeck A, Achenbach S, Layritz C, Eisentopf J, Hecker F, Pflederer T, et al. Image quality of ultra-low radiation exposure coronary CT angiography with an effective dose< 0.1 mSv using high-pitch spiral acquisition and raw data-based iterative reconstruction. European radiology. 2013;23:597–606.
6. Nakaura T, Kidoh M, Sakaino N, Utsunomiya D, Oda S, Kawahara T, et al. Low contrast-and low radiation dose protocol for cardiac CT of thin adults at 256-row CT: usefulness of low tube voltage scans and the hybrid iterative reconstruction algorithm. The international journal of cardiovascular imaging. 2013;29:913–23.
7. Nagayama Y, Iwashita K, Maruyama N, Uetani H, Goto M, Sakabe D, et al. Deep learning-based reconstruction can improve the image quality of low radiation dose head CT. European Radiology. 2023;33(5):3253–65.
8. Vassileva J, Rehani M. Diagnostic reference levels. AJR Am J Roentgenol. 2015;204(1):W1-3.
9. Vañó E, Miller DL, Martin CJ, Rehani MM, Kang K, Rosenstein M, et al. ICRP publication 135: diagnostic reference levels in medical imaging. Annals of the ICRP. 2017;46(1):1–144.
10. Seibert JA. Tradeoffs between image quality and dose. Pediatric radiology. 2004;34:S183–95.
11. Strauss KJ, Goske MJ, Kaste SC, Bulas D, Frush DP, Butler P, et al. Image gently: ten steps you can take to optimize image quality and lower CT dose for pediatric patients. American Journal of Roentgenology. 2010;194(4):868–73.
12. Power SP, Moloney F, Twomey M, James K, O'Connor OJ, Maher MM. Computed tomography and patient risk: Facts, perceptions and uncertainties. World journal of radiology. 2016;8(12):902.
13. Brody AS, Frush DP, Huda W, Brent RL, Radiology S on. Radiation risk to children from computed tomography. Pediatrics. 2007;120(3):677–82.
14. Omer H, Alameen S, Mahmoud WE, Sulieman A, Nasir O, Abolaban F. Eye lens and thyroid gland radiation exposure for patients undergoing brain computed tomography examination. Saudi Journal of Biological Sciences. 2021;28(1):342–6.
15. Tarkiainen J, Nadhum M, Heikkilä A, Rinta-Kiikka I, Joutsen A. Radiation dose of the eye lens in CT examinations of the brain in clinical practice—the effect of radiographer training to optimise gantry tilt and scan length. Radiation Protection Dosimetry. 2023;199(5):391–8.
16. Tien HC, Tremblay LN, Rizoli SB, Gelberg J, Spencer F, Caldwell C, et al. Radiation exposure from diagnostic imaging in severely injured trauma patients. Journal of Trauma and Acute Care Surgery. 2007;62(1):151–6.
17. Lin EC. Radiation risk from medical imaging. In: Mayo Clinic Proceedings. Elsevier; 2010. p. 1142–6.
18. Smith-Bindman R, Kwan ML, Marlow EC, Theis MK, Bolch W, Cheng SY, et al. Trends in use of medical imaging in US health care systems and in Ontario, Canada, 2000-2016. Jama. 2019;322(9):843–56.
19. Geise RA. Computed tomography: physical principles, clinical applications, and quality control. Radiology. 1995;194(3):782–782.
20. Mayo-Smith WW, Hara AK, Mahesh M, Sahani DV, Pavlicek W. How I do it: managing radiation dose in CT. Radiology. 2014;273(3):657–72.
21. McNitt-Gray MF. AAPM/RSNA physics tutorial for residents: topics in CT: radiation dose in CT. Radiographics. 2002;22(6):1541–53.
22. Raman SP, Mahesh M, Blasko RV, Fishman EK. CT scan parameters and radiation dose: practical advice for radiologists. Journal of the American College of Radiology. 2013;10(11):840–6.
23. Kim JH, Yoon HJ, Lee E, Kim I, Cha YK, Bak SH. Validation of deep-learning image reconstruction for low-dose chest computed tomography scan: emphasis on image quality and noise. Korean journal of radiology. 2021;22(1):131.
24. Padole AM, Sagar P, Westra SJ, Lim R, Nimkin K, Kalra MK, et al. Development and validation of image quality scoring criteria (IQSC) for pediatric CT: a preliminary study. Insights into imaging. 2019;10:1–11.
25. Scholtz JE, Kaup M, Kraft J, Nöske EM, Scheerer F, Schulz B, et al. Objective and subjective image quality of primary and recurrent squamous cell carcinoma on head and neck low-tube-voltage 80-kVp computed tomography. Neuroradiology. 2015;57:645–51.
26. Tamura A, Mukaida E, Ota Y, Kamata M, Abe S, Yoshioka K. Superior objective and subjective image quality of deep learning reconstruction for low-dose abdominal CT imaging in comparison with model-based iterative reconstruction and filtered back projection. The British Journal of Radiology. 2021;94:20201357.

27. Pahn G, Skornitzke S, Schlemmer HP, Kauczor HU, Stiller W. Toward standardized quantitative image quality (IQ) assessment in computed tomography (CT): A comprehensive framework for automated and comparative IQ analysis based on ICRU Report 87. Physica Medica. 2016;32(1):104–15.
28. Hussain FA, Mail N, Shamy AM, Alghamdi S, Saoudi A. A qualitative and quantitative analysis of radiation dose and image quality of computed tomography images using adaptive statistical iterative reconstruction. Journal of applied clinical medical physics. 2016;17(3):419–32.
29. Mail TB. Catphan® 700 Manual. 2013;
30. Goodenough D, Levy J, Kristinsson S, Fredriksson J, Olafsdottir H, Healy A. Method and phantom to study combined effects of in-plane (x, y) and z-axis resolution for 3D CT imaging. Journal of Applied Clinical Medical Physics. 2016;17(5):440–52.
31. Neusoft Medical Systems Co., Ltd. Nuesoft NeuViz 128 Computed Tomography [Internet]. 2016. Available from: https://intermed1.com/wp-content/uploads/2019/03/NeuViz128_brochure_0716.pdf
32. Dillon C, Davidson C, Hernandez D. 2017 Computed Tomography Quality Control Manual. American College of Radiology; 2017.
33. Anam C, Amilia R, Naufal A, Budi WS, Maya AT, Dougherty G. The automated measurement of CT number linearity using an ACR accreditation phantom. Biomedical Physics & Engineering Express. 2022;9(1):017002.
34. McCollough CH, Bruesewitz MR, McNitt-Gray MF, Bush K, Ruckdeschel T, Payne JT, et al. The phantom portion of the American College of Radiology (ACR) Computed Tomography (CT) accreditation program: Practical tips, artifact examples, and pitfalls to avoid. Med Phys. 2004 Aug 19;31(9):2423–42.
35. Friedman SN, Fung GS, Siewerdsen JH, Tsui BM. A simple approach to measure computed tomography (CT) modulation transfer function (MTF) and noise-power spectrum (NPS) using the American College of Radiology (ACR) accreditation phantom. Medical physics. 2013;40(5):051907.
36. Takenaga T, Katsuragawa S, Goto M, Hatemura M, Uchiyama Y, Shiraishi J. Modulation transfer function measurement of CT images by use of a circular edge method with a logistic curve-fitting technique. Radiological physics and technology. 2015;8:53–9.
37. Judy PF. The line spread function and modulation transfer function of a computed tomographic scanner. Medical physics. 1976;3(4):233–6.
38. Bissonnette JP, Moseley DJ, Jaffray DA. A quality assurance program for image quality of cone-beam CT guidance in radiation therapy. Medical physics. 2008;35(5):1807–15.
39. STRÅLSKYDDSFRÅGOR NRO. A Quality Control Programme for Radiodiagnostic Equipment: Acceptance tests.
40. Li Y, Jiang Y, Liu H, Yu X, Chen S, Ma D, et al. A phantom study comparing low-dose CT physical image quality from five different CT scanners. Quantitative Imaging in Medicine and Surgery. 2022;12(1):766.
41. Bellesi L, Wyttenbach R, Gaudino D, Colleoni P, Pupillo F, Carrara M, et al. A simple method for low-contrast detectability, image quality and dose optimisation with CT iterative reconstruction algorithms and model observers. European radiology experimental. 2017;1:1–10.
42. Anam C, Amilia R, Naufal A, Sutanto H, Dwihapsari Y, Fujibuchi T, et al. Impact of Noise Level on the Accuracy of Automated Measurement of CT Number Linearity on ACR CT and Computational Phantoms. Journal of Biomedical Physics & Engineering. 2023;13(4):353.
43. Romans LE. Computed Tomography for Technologist, A Comprehensive Text. Wolter Kluwer Health. Lippincott Williams and Wilkins: Maryland dan Pensylvania; 2011.
44. BAXTER BS, SORENSON JA. Factors affecting the measurement of size and CT number in computed tomography. Investigative radiology. 1981;16(4):337–41.
45. Cann CE. Quantitative CT for determination of bone mineral density: a review. Radiology. 1988;166(2):509–22.
46. McCollough CH, Bruesewitz MR, McNitt-Gray MF, Bush K, Ruckdeschel T, Payne JT, et al. The phantom portion of the American College of Radiology (ACR) computed tomography (CT) accreditation program: practical tips, artifact examples, and pitfalls to avoid. Medical physics. 2004;31(9):2423–42.
47. Rueckel J, Stockmar M, Pfeiffer F, Herzen J. Spatial resolution characterization of a X-ray microCT system. Applied Radiation and Isotopes. 2014;94:230–4.
48. Grimmer R, Krause J, Karolczak M, Lapp R, Kachelriess M. Assessment of spatial resolution in CT. In: 2008 IEEE Nuclear Science Symposium Conference Record. IEEE; 2008. p. 5562–6.

49. Roa AMA, Andersen HK, Martinsen ACT. CT image quality over time: comparison of image quality for six different CT scanners over a six-year period. Journal of applied clinical medical physics. 2015;16(2):350–65.
50. Gulliksrud K, Stokke C, Martinsen ACT. How to measure CT image quality: variations in CT-numbers, uniformity and low contrast resolution for a CT quality assurance phantom. Physica Medica. 2014;30(4):521–6.
51. Manson EN, Fletcher JJ, Della Atuwo-Ampoh V, Addison EK, Schandorf C, Bambara L. Assessment of some image quality tests on a 128 slice computed tomography scanner using a Catphan700 phantom. Journal of Medical Physics/Association of Medical Physicists of India. 2016;41(2):153.
52. Ghetti C, Ortenzia O, Serreli G. CT iterative reconstruction in image space: a phantom study. Physica medica. 2012;28(2):161–5.